ICAS PAPER No. 72-10

Influence of Discontinuity Stress on Main Propellant Tankage of a Space Shuttle Orbiter

by
Hans R. Meyer–Piening, Head, Section "Dynamic Stability"
ERNO, Raumfahrttechnik GmbH, Bremen, West Germany

and

John H. Dutton, Project Strength Engineer
McDonnell Douglas Astronautics Company–East
St. Louis, Missouri, USA

The Eighth Congress of the International Council of the Aeronautical Sciences

INTERNATIONAAL CONGRESCENTRUM RAI–AMSTERDAM, THE NETHERLANDS
AUGUST 28 TO SEPTEMBER 2, 1972

Price: 3. Dfl.

INFLUENCE OF DISCONTINUITY STRESSES ON MAIN PROPELLANT TANKAGE OF A SPACE SHUTTLE ORBITER

HANS-R. MEYER-PIENING
Erno Raumfahrttechnik Gmbh, Bremen, West Germany
and
JOHN H. DUTTON
McDonnell Douglas Corporation, St. Louis, Missouri, U.S.A.

Abstract

A general closed form solution is given for the calculation of local stresses in cylindrical axial load carrying pressure vessels which are heavily stiffened in the axial direction and circumferentially restrained by closely spaced ring stiffeners. The ring stiffeners are treated as discrete stiffeners and are allowed to have a temperature variation throughout the radial extension of the stiffener and different material properties compared with those of the vessel.

Numerical results are presented for representative LO_2 and LH_2 main propellant tank geometries and loads for a fully reusable Space Shuttle Orbiter configuration studied by the McDonnell Douglas Corporation (MDC) under a NASA-funded Phase B Contract. A parametric study is included in which stiffener spacings and cross-sections are varied.

List of Symbols

a	radius of neutral surface, (figure 2)
A, A_s	cross section area of ringstiffeners, (figure 3)
b	lateral thickness of axial stiffener, (figure 3)
$\bar{c}$, ch	abbreviations, equation (35)
$C_1 - C_4$	coefficients of displacement function, equations (28), (29)
D	extensional stiffness, equation (9)
D_x	extensional stiffness, equation (8)
D_ϕ	extensional stiffness, equation (13)
D_M	coefficient, equation (17)
$\widetilde{D}$	resulting extensional stiffness, equations (26), (27)
e, e'	radial distance from neutral surface, (figure 2)
E	Young's modulus
EX, EMX	abbreviations, equation (35)
h	radial extension of axial stiffener from middle surface of tank wall
I	resulting moment of inertia
K	bending stiffness, equation (18)
K_x	bending stiffness, equation (10)
K_ϕ	bending stiffness, equation (14)
L	spacing of main ring stiffener (figure 3)
M_x	distributed bending moment
$\bar{N}_x$	prescribed axial line load
$\widetilde{N}_x$	resulting axial line load, equations (26), (27)
N_ϕ	circumferential line load
P_i	internal pressure
Q_x	shear force of shell
R	inner radius of ring stiffener ($R = a - e + t/2$)
s	spacing of axial stiffeners
$\bar{s}$, sh	abbreviations, equation (35)
t	wall thickness of tank, figure (4)
t_R	web thickness of main ring stiffener
ΔT_i	temperature difference of area A_i of main ring stiffener
ΔT_s	temperature difference of tank wall
u	axial displacement
w	radial displacement
w_p	coefficient of displacement function, equation (30)
x	axial coordinate
z	radial coordinate
α_T	thermal expansion coefficient
α	parameter, equation (31)
β, $\bar{\beta}$	parameters, equations (32), (33)
ϵ_x, ϵ_ϕ	axial and circumferential strains
ν	Poisson's ratio
σ_x, σ_ϕ	axial and circumferential stresses in shells
$\sigma_x(s)$	axial stress in axial stiffener
Γ, Ξ	coefficients, equations (34), (42)
$(\ )'$	differentiation with respect to (x/a)

I. Introduction

The main liquid oxygen and liquid hydrogen tanks of a fully reusable Space Shuttle Orbiter configuration (figure 1a) studied by MDC, a NASA-funded Phase B study contract, were designed integral with the primary body structure. An orthogonally stiffened pressure vessel design for these tanks (figure 1b) provided high axial buckling efficiency, discrete support for the thermal protection system, and frame continuity with upper frames supporting longerons resulting an overall highly efficient structural arrangement.

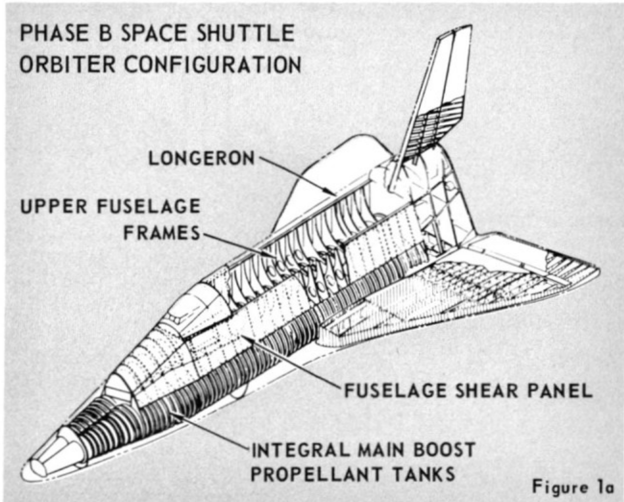

Figure 1a

The resulting structure is relatively flexible with regard to circumferential stretching in between the ring stiffeners and relatively stiff with regard to axial bending of the wall.

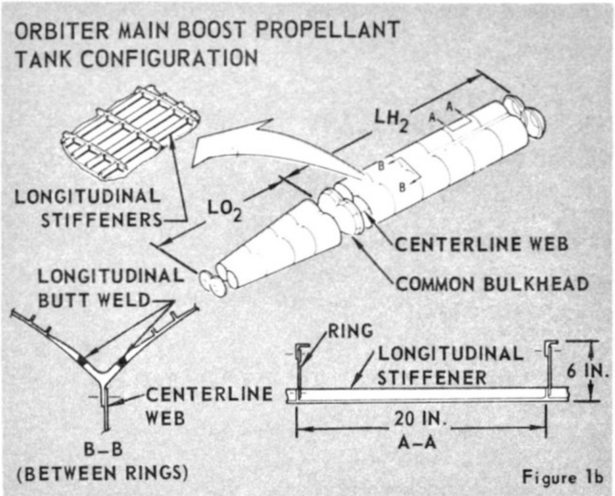

Figure 1b

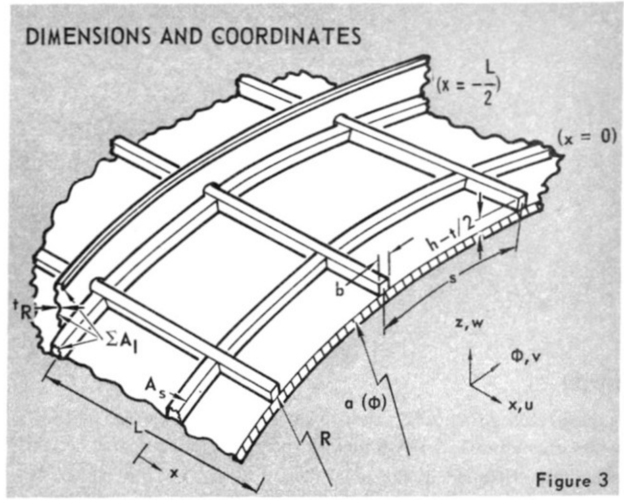

Figure 3

This results in high bending stresses in the outer fibers of the axial stiffeners at each ring stiffener. Careful attention to detail design to minimize structural weight impact was required in those areas where high compressive stress could cause local crippling of the stiffeners.

The derivation of the equations is based on Flügge's derivation, given in reference 1 for cylindrical pressure vessels with closely spaced ring stiffeners. The equations are modified to account for different bending and stretching properties in the axial and circumferential direction.

For the evaluation of bending stresses in the axial stiffener, the stiffeners are treated as being in a discrete arrangement.

II. Basic Equations

The basic equations are derived in accordance with the derivation given by Flügge in reference 1. It is assumed that the bending stiffness does not vary along the axial and circumferential direction of the vessel and that the applied load is axisymmetric. For the region of maximum vehicle axial stresses, the variations of stiffenesses can be assumed to be negligible, as can be the variations of stresses in the circumferential direction.

The axisymmetric strains are given by

$$\epsilon_x = \frac{u'}{a} - z\frac{w''}{a^2} \quad (1)$$

$$\epsilon_\phi = \frac{w}{a+z} \quad (2)$$

(compare figures 2 and 3).

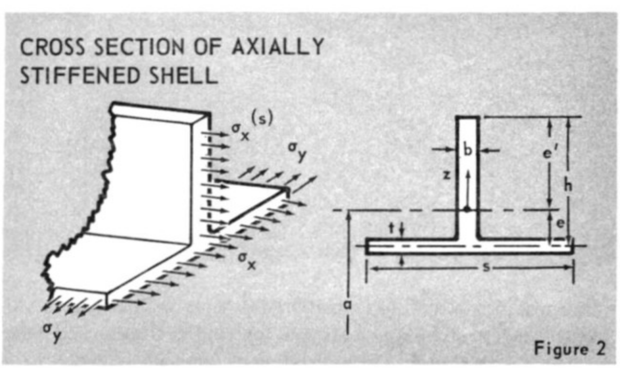

Figure 2

The stresses are given by

$$\sigma_x = \frac{E}{1-\nu^2}(\epsilon_x + \nu\epsilon_\phi) \quad (3)$$

$$\sigma_\phi = \frac{E}{1-\nu^2}(\epsilon_\phi + \nu\epsilon_x) \quad (4)$$

In the axial stiffeners σ_ϕ is equal to zero, and therefore,

$$\sigma_x^{(s)} = E\,\epsilon_x = E\left(\frac{u'}{a} - z\frac{w''}{a^2}\right) \quad (5)$$

For the net running load in axial direction one gets

$$N_x = \bar{N}_x = \int_{-e-t/2}^{-e+t/2} \sigma_x \frac{(a+z)}{a}\,dz + \frac{b}{s}\int_{-e+t/2}^{e'} \sigma_x^{(s)} \frac{a+z}{a}\,dz$$

$$= \frac{E}{a(1-\nu^2)}\int_{-e-t/2}^{-e+t/2} \left(\frac{u'}{a} - z\frac{w''}{a^2} + \nu\frac{w}{a+z}\right)(a+z)\,dz$$

$$+ \frac{Eb}{a\cdot s}\int_{-e+t/2}^{e'} \left(\frac{u'}{a} - z\frac{w''}{a^2}\right)(a+z)\,dz \quad (6)$$

or finally,

$$\bar{N}_x = \frac{D_x}{a}u' + \nu\frac{D}{a}w + \frac{K_x}{a^3}w'' \quad (7)$$

where

$$D_x = E\left\{\frac{t(1-e/a)}{1-\nu^2} + \frac{bh}{s}\left[1 + \frac{e'-e}{2a} - \frac{t}{2h}\left(1 - \frac{e}{a} + \frac{t}{4a}\right)\right]\right\} \quad (8)$$

$$D = \frac{E\,t}{1-\nu^2} \quad (9)$$

$$K_x = \frac{E}{1-\nu^2}\left(\frac{t^3}{12} + e^2 t - aet\right)\left[1 - \frac{b}{2s}(1-\nu^2)\right] - \frac{Ebt^2}{8s}(a-2e)$$

$$+ \frac{Eb}{s}\left[\frac{ah}{2}(e'-e) + \frac{(e')^3 + e^3}{3}\right] \quad (10)$$

For the circumferential direction the corresponding expression becomes

$$N_\phi \frac{a(1-\nu^2)}{E} = \int_{-e-t/2}^{-e+t/2} (\epsilon_\phi + \nu \epsilon_x)(a+z)dz$$

$$= \int_{-e-t/2}^{-e+t/2} (w + \nu u' \frac{a+z}{a} - \nu z(a+z)\frac{w''}{a^2})dz \tag{11}$$

or

$$N_\phi = \nu \frac{D\phi}{a} u' + \frac{D}{a} w - \nu \frac{K_\phi}{a^3} w'' \tag{12}$$

where

$$D_\phi = \frac{Et}{1-\nu^2}(1-e/a) \tag{13}$$

$$K_\phi = \frac{E}{1-\nu^2}(\frac{t^3}{12} + e^2 t - eat) \tag{14}$$

For the bending moment the following expression is derived

$$M_x = \int_{-e-t/2}^{-e+t/2} \sigma_x (1 + z/a) z dz - \int_{-e+t/2}^{e'} \sigma_x^{(s)} (1 + z/a) z dz \tag{15}$$

$$= -\frac{E}{1-\nu^2} \int_{-e-t/2}^{-e+t/2} [\frac{zu'}{a} + \frac{u'}{a^2} z^2 - z^2 \frac{w''}{a^2} - \frac{z^3 w''}{a^3} + \frac{\nu z w}{a}]dz$$

$$-E \int_{-e+t/2}^{e'} [\frac{u'}{a} z + \frac{u'}{a^2} z^2 - \frac{w''}{a^2} z^2 - \frac{w''}{a^3} z^3]dz$$

which results in

$$M_x = D_M u' + \frac{K}{a^2} w'' + \nu \frac{e}{a} D w \tag{16}$$

where

$$D_M = \frac{E}{1-\nu^2} \{ (\frac{et}{a} - \frac{e^2 t}{a^2} - \frac{t^3}{12a^2})[1 - \frac{b(1-\nu^2)}{2s}]$$

$$- \frac{b(1-\nu^2)}{s} [\frac{h(e'-e)}{2a} + \frac{(e')^3 + e^3}{3a^2} + \frac{et^2}{4a^2} - \frac{t^2}{8a}] \tag{17}$$

$$K = \frac{E}{1-\nu^2} \{ (e^2 t + \frac{t^3}{12} - \frac{e^3 t}{a} - \frac{et^3}{4a}) [1 - \frac{b(1-\nu^2)}{2s}] \}$$

$$+ \frac{Eb}{s} [\frac{et^2}{4} - \frac{3}{8} \frac{e^2 t^2}{a} - \frac{t^4}{64a} + \frac{(e')^3 + e^3}{3} + \frac{(e')^4 - e^4}{4a}] \tag{18}$$

The coefficient D_M, equation (17), has to vanish since for $w'' = w = 0$, M_x is required to be zero for all values of u'.

From equation (17), i.e., from the condition $D_M = 0$, the value of e can be calculated. After replacing e′ by h - e the evaluation leads to a quadratic equation:

$$e = \frac{\bar{B}}{2\bar{A}} (1 - \sqrt{1 - \frac{4 \bar{C} \bar{A}}{\bar{B}^2}}) \tag{19}$$

where

$$\bar{A} = h + t[\frac{s}{b(1-\nu^2)} - \frac{1}{2}]$$

$$\bar{B} = ah + h^2 - \frac{t^2}{4} + ta[\frac{s}{b(1-\nu^2)} - \frac{1}{2}] \tag{20}$$

$$\bar{C} = \frac{ah^2}{2} + \frac{h^3}{3} - \frac{at^2}{8} + \frac{t^3}{12}[\frac{s}{b(1-\nu^2)} - \frac{1}{2}]$$

The numerical evaluation related to Space Shuttle Orbiter tank geometry reveals that the term $4 \cdot \bar{C} \cdot \bar{A}/\bar{B}^2$ is very small compared with unity (≈0.2 percent) and, hence, e may be obtained from

$$e \approx \frac{\bar{C}}{\bar{B}} \tag{21}$$

$$e' = h - \frac{\bar{C}}{\bar{B}} \tag{22}$$

Now the following equations have to be solved. For equilibrium of radial forces, see figure 4a and 4b,

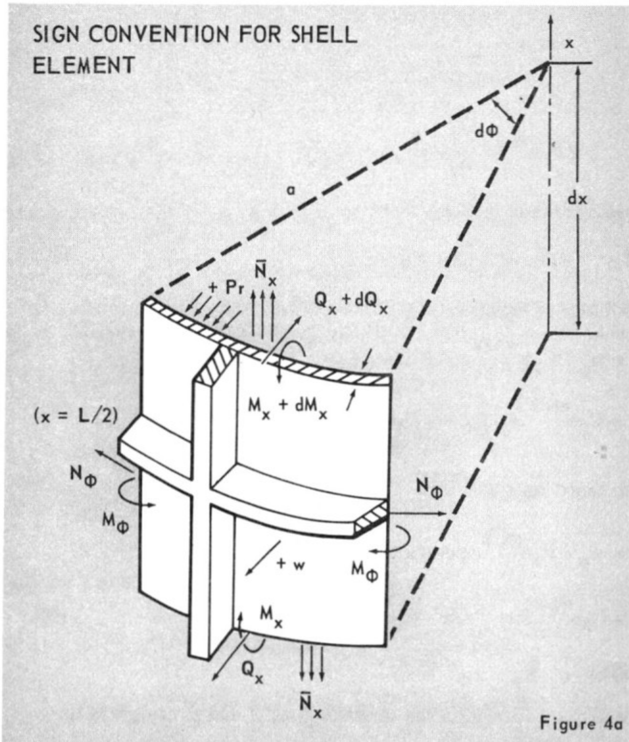

Figure 4a

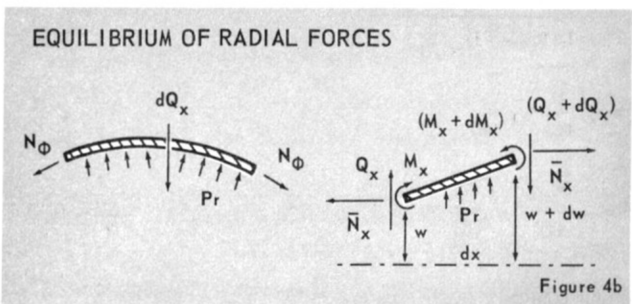

Figure 4b

$$M_x'' + aN_\phi - \bar{N}_x w'' = p_r a^2 \qquad (23)$$

where

$$\bar{N}_x = \frac{D_x}{a} u' + \nu \frac{D}{a} w - \frac{K_x}{a^3} w'' \qquad (7)$$

$$N_\phi = \nu \frac{D_\phi}{a} u' + \frac{D}{a} w - \frac{K_\phi}{a^3} w'' \qquad (12)$$

$$M_x = \frac{K}{a^2} w'' + \nu \frac{e}{a} D\, w \qquad (16)$$

or, using Equation (7),

$$M_x'' = \frac{K}{a^2} w'''' + \nu \frac{e}{a} D\, w'' \qquad (24)$$

Elimination of u' from the equation for $\bar{N}_x$ and N_ϕ yields

$$aN_\phi = \nu \frac{D_\phi}{D_x} a\, \bar{N}_x + wD\left(1-\nu^2 \frac{D_\phi}{D_x}\right) - \nu w''\left(\frac{K_\phi}{a^2} - \frac{D_\phi\, K_x}{D_x\, a^2}\right) \qquad (25)$$

and after substitution in Equation (23) one finds

$$\frac{K}{a^2} w'''' - \left[\bar{N}_x + \nu\left(\frac{K_\phi}{a^2} - \frac{D_\phi K_x}{D_x a^2}\right) - \nu \frac{e}{a} D\right] w'' + D\left(1-\nu^2 \frac{D_\phi}{D_x}\right) w \qquad (26)$$

$$= p_r\, a^2 - \nu \frac{D_\phi}{D_x} a\bar{N}_x$$

Equation (26) is of the form

$$EI\, w'''' - \tilde{N}_x\, w'' + \tilde{D}\, w = \tilde{p} \qquad (27)$$

The solution of Equation (27) is known to be

$$w = w_p + C_1 e^{\alpha x/a} \cos \beta\, x/a + C_2 e^{-\alpha x/a} \cos \beta x/a$$

$$+ C_3 e^{\alpha x/a} \sin \beta x/a + C_4 e^{-\alpha x/a} \sin \beta x/a \qquad (28)$$

for the case: $\tilde{N}_x < 2\sqrt{\tilde{D} \cdot EI}$

and

$$w = w_p + C_1 e^{\alpha x/a} \cosh \bar{\beta}\, x/a + C_2 e^{-\alpha x/a} \cosh \bar{\beta} x/a$$

$$+ C_3 e^{\alpha x/a} \sinh \bar{\beta} x/a + C_4 e^{-\alpha x/a} \sinh \bar{\beta}\, x/a \qquad (29)$$

for the case: $\tilde{N}_x > 2\sqrt{\tilde{D} \cdot EI}$

In the above expression the terms w_p, α, β and $\bar{\beta}$ are given as

$$w_p = \frac{p_r\, a^2 - \nu(D_\phi/D_x) a\, \bar{N}_x}{D(1 - \nu^2\, D_\phi/D_x)} \qquad (30)$$

$$\alpha^2 = \sqrt{\frac{\tilde{D}}{4EI}} + \frac{\tilde{N}_x}{4EI} \qquad (31)$$

$$\beta^2 = -\frac{\tilde{N}_x}{4EI} + \sqrt{\frac{\tilde{D}}{4EI}} \quad \text{and } \bar{\beta}^2 = -\beta^2 \qquad (32), (33)$$

The four boundary conditions are

$$\begin{aligned} \mid x = 0: \quad & w' = 0 \\ & w''' = \Xi\, w(x = 0) \\ \mid x = L/2 \quad & w' = 0 \\ & w''' = \Gamma \cdot w(x = L/2) \end{aligned} \qquad (34)$$

where w(L/2) is identical to the radial deflection of the ring stiffener and Γ and Ξ are factors to be discussed later which relate the deflection of the tank wall to the resulting radial line load Q_x.

For reasons of simplicity the following abbreviations will be introduced

$$EX = e^{\alpha L/2a},\ EM_x = e^{-\alpha L/2a}$$

$$\bar{c} = \cos \beta L/2a,\ \bar{s} = \sin \beta L/2a \qquad (35)$$

$$ch = \cosh \beta L/2a,\ sh = \sinh \beta L/2a$$

Then the four constants C_1 - C_4 can be found by solving the set of equations represented in table 1.

From figure 3 the following relation, already contained in equation (23), can be found

$$\frac{dM_x}{d_x} - \bar{N}_x \frac{dw}{dr} - Q_x = 0 \qquad (36)$$

or

$$M_x' - \bar{N}_x w' - a\, Q_x = 0 \qquad (37)$$

Introduction of equation (16) into equation (37) yields

$$\frac{K}{a^2} w''' - \nu \frac{e}{a} D\, w' - \bar{N}_x\, w' = aQ_x \qquad (38)$$

At x = L/2 and x = 0 the slope w' is required to vanish, see equation (34), and, hence, equation (38) becomes

$$\frac{K}{a^2} w''' = aQ_x \qquad (39)$$

Owing to the assumed linear elasticity of the ring stiffener the radial line load Q_x is directly related to the radial displacement w.

In the following discussion it will be assumed that an additional ring stiffener will be attached to the tank wall at x = 0, i.e., $\Xi \neq 0$ in equation (34). The cross section of the ring stiffener at x = L/2 is $A = \Sigma A_i$ and that of the ring stiffener at x = 0 is A_s, whereby $A_s < A$.

The radial line load acting at the ring stiffener is twice the load given by equation (36), since Q_x is transferred to the ring stiffener from both sides of the shell

$$Q_x \big|_{x = L/2} = \frac{1}{2} w_{(x = L/2)} \frac{EA}{R^2} \qquad (40a)$$

$$Q_x \big|_{x = 0} = -\frac{1}{2} w_{(x = 0)} \frac{EA_s}{R^2} \qquad (40b)$$

Finally, Equations (39) and (40) yield the condition

TABLE I

SET OF EQUATIONS FOR DETERMINATION OF $C_1 - C_4$

CASE I, $N_x < 2\sqrt{\tilde{D}\,EI}$

$$\begin{bmatrix} \alpha & -\alpha & \beta & \beta \\ (\alpha\bar{c} - \beta\bar{s})E_x & (-\alpha\bar{c} - \beta\bar{s})EM_x & (\alpha\bar{s} + \beta\bar{c})E_x & (-\alpha\bar{s} + \beta\bar{c})EM_x \\ AB - \Xi & -AB - \Xi & -BA & -BA \\ [(AB-\Gamma)\bar{c} + BA\bar{s}]E_x & [(-AB-\Gamma)\bar{c} + BA\bar{s}]EM_x & [(AB-\Gamma)\bar{s} - BA\bar{c}]E_x & [(-AB-\Gamma)\bar{s} - BA\bar{c}]EM_x \end{bmatrix} \begin{Bmatrix} C_1 \\ C_2 \\ C_3 \\ C_4 \end{Bmatrix} = \begin{Bmatrix} 0 \\ 0 \\ \Xi \cdot w_p \\ \Gamma \cdot \bar{w}_p \end{Bmatrix}$$

where $AB = \alpha^3 - 3\alpha\beta^2 \quad BA = \beta^3 - 3\alpha^2\beta$

CASE II, $N_x > 2\sqrt{\tilde{D} \cdot EI}$

$$\begin{bmatrix} \alpha & -\alpha & \bar{\beta} & \bar{\beta} \\ (\alpha ch - \bar{\beta} sh)E_x & (-\alpha ch + \bar{\beta} sh)EM_x & (\alpha sh + \bar{\beta} ch)E_x & (-\alpha sh + \bar{\beta} ch)EM_x \\ AB - \Xi & -AB - \Xi & BA & BA \\ [(AB-\Gamma)ch + BA sh]E_x & [(-AB-\Gamma)ch + BA sh]EM_x & [(AB-\Gamma)sh + BA ch]E_x & [(-AB-\Gamma)sh + BA ch]EM_x \end{bmatrix} \begin{Bmatrix} C_1 \\ C_2 \\ C_3 \\ C_4 \end{Bmatrix} = \begin{Bmatrix} 0 \\ 0 \\ \Xi w_p \\ \Gamma \bar{w}_p \end{Bmatrix}$$

where $AB = \alpha^3 + 3\alpha\bar{\beta}^2$ and $BA = \bar{\beta}^3 + 3\alpha^2\bar{\beta}$

$\bar{w}_p = w_p$ for zero temperature difference between ring stiffeners and tank wall.

$$\frac{K}{a^2} w'''_{(x = L/2)} = \frac{EAa}{2R^2} w_{(x = L/2)} \qquad (41a)$$

$$\frac{K}{a^2} w'''_{(x = 0)} = \frac{-E A_s a}{2R^2} w_{(x = 0)} \qquad (41b)$$

from which the values of Γ and Ξ in equation (34) and in table 1 are directly obtained to be

$$\Gamma = \frac{EAa^3}{2KR^2}, \Xi = \frac{-E A_s a^3}{2KR^2} \qquad (42a, b)$$

In equation (41) the function w, according to equation (28) or (29), and its third derivative with respect to (x/a), w‴, has to be introduced in order to find the fourth equation in table 1. From the set of equations given in table 1 the four constants C_1 - C_4 can be obtained. For the case $A_s = 0$ the calculations can be simplified by setting $C_1 = C_2$ and $C_3 = -C_4$, which for this case satisfies the equations contained in row 1 and row 3 in table 1. This special solution corresponds to hyperbolic functions instead of to the assumed exponential functions.

The case $\tilde{N}_x = 2 \cdot \sqrt{\tilde{D} \cdot EI}$ will not be discussed, since it may be regarded as an exceptional case and may be avoided by a slight modification of the value of $\tilde{N}_x$.

In order to evaluate the resulting stresses, it is suitable to calculate u′, w and w″ for each desired station along the axial coordinate x.

From equation (7) we have

$$\frac{u'}{a} = \frac{\bar{N}_x}{D_x} - \nu \frac{D}{a} w + \frac{K_x}{a^3} w'' \qquad (43)$$

where, for Case I, ($\tilde{N}_x < 2\sqrt{\tilde{D}\,EI}$)

$$w = w_p + C_1 e^{\alpha x/a} \cos \beta x/a + C_2 e^{-\alpha x/a} \cos \beta x/a + C_3 e^{\alpha x/a} \sin \beta x/a + C_4 e^{-\alpha x/a} \sin \beta x/a \qquad (28)$$

$$\begin{aligned} w'' = {} & C_1 [(\alpha^2 - \beta^2) \cos \beta x/a - 2\alpha\beta \sin \beta x/a] e^{\alpha x/a} \\ & + C_2 [(\alpha^2 - \beta^2) \cos \beta x/a + 2\alpha\beta \sin \beta x/a] e^{-\alpha x/a} \\ & + C_3 [(\alpha^2 - \beta^2) \sin \beta x/a + 2\alpha\beta \cos \beta x/a] e^{\alpha x/a} \\ & + C_4 [(\alpha^2 - \beta^2) \sin \beta x/a - 2\alpha\beta \cos \beta x/a] e^{-\alpha x/a} \end{aligned} \qquad (44)$$

and for Case II ($N_x > 2\sqrt{\tilde{D} EI}$)

$$w = w_p + C_1 e^{\alpha x/a} \cosh \bar{\beta} x/a + C_2 e^{\alpha x/a} \cosh \bar{\beta} x/a + C_3 e^{\alpha x/a} \sinh \bar{\beta} x/a + C_4 e^{-\alpha x/a} \sinh \bar{\beta} x/a \qquad (29)$$

$$\begin{aligned} w'' = {} & C_1 [(\alpha^2 + \bar{\beta}^2) \cosh \bar{\beta} x/a + 2\alpha\bar{\beta} \sinh \bar{\beta} x/a] e^{\alpha x/a} \\ & + C_2 [(\alpha^2 + \bar{\beta}^2) \cosh \bar{\beta} x/a - 2\alpha\bar{\beta} \sinh \bar{\beta} x/a] e^{-\alpha x/a} \\ & + C_3 [(\alpha^2 + \bar{\beta}^2) \sinh \bar{\beta} x/a + 2\alpha\bar{\beta} \cosh \bar{\beta} x/a] e^{\alpha x/a} \\ & + C_4 [(\alpha^2 + \bar{\beta}^2) \sinh \bar{\beta} x/a - 2\alpha\bar{\beta} \cosh \bar{\beta} x/a] e^{-\alpha x/a} \end{aligned} \qquad (45)$$

From Equations (1) through (5) the following formulas are derived

– Max bending stress at outer fiber of axial stiffener

$$\sigma_x^{(s)} = E\left(\frac{u'}{a} - e'\frac{w''}{a^2}\right) \qquad (46)$$

– Max bending stress at inner shell radius

$$\sigma_x = \frac{E}{1-\nu^2}\left(\frac{u'}{a} + (e + t/2)\frac{w''}{a-e-t/2}\right) \qquad (47)$$

– Hoop stress in the shell

$$\sigma_\phi = \frac{E}{1-\nu^2}\left[\frac{w}{a-e\pm\frac{t}{2}} + \nu\frac{u'}{a} + \nu\left(e\mp\frac{t}{2}\right)\frac{w''}{a^2}\right] \qquad (48)$$

Hoop stress in the ring sitffener

$$\sigma_\phi^{(R)} = E\,\frac{w_{(x = L/2)}}{a-e+t} \qquad (49)$$

– Radial stress in the ring stiffener

$$\sigma_R^{(R)} = \frac{E\,A\,w_{(t = L/2)}}{2(a-e+t)^2\,t_R} \qquad (50)$$

III. Consideration of Temperature Gradient

In the following discussion it will be assumed that the ring stiffener, owing to heat conduction, has a certain temperature gradient. The thermal deflection of the ring stiffener may be calculated from

$$w_T^{(R)} = (a+t)\,\alpha_T\,\frac{\Sigma A_i\,\Delta T_i}{\Sigma A_i} \qquad (51)$$

where A_i designates a certain portion of the ring stiffener cross section at temperature ΔT_i, whereas the thermal deflection of the remaining tank wall is given by

$$w_T^{(s)} = a\,\alpha_T\,\Delta T_s \qquad (52)$$

Since $w_T^{(R)}$ may be different from $w_T^{(s)}$, equation (41) has to be modified in order to match the new compatibility condition

$$Q_x = \frac{E\,A}{2R^2}\left[w - \left(a-e+\frac{t}{2}\right)\alpha_T\left(\frac{\Sigma A_i\,\Delta T_i}{\Sigma A_i} - \Delta T_s\right)\right] \qquad (53)$$

The only difference in table 1 will be that w_p has to be replaced by $\bar{w}_p$ where

$$\bar{w}_p = w_p - \left(a-e+\frac{t}{2}\right)\alpha_T\left(\frac{\Sigma A_i\,\Delta T_i}{\Sigma A_i} - \Delta T_s\right) \qquad (54)$$

For the determination of the radial deflection w has to be replaced by $\bar{w}$, where

$$\bar{w} = w + \alpha_T\,a\,\Delta T_s \qquad (55)$$

and $w_{(x = L/2)}$ in equations (46) and (47) has to be replaced by $w_{(x = L/2)}$ where

$$\bar{w}(x = L/2) = w(x = L/2) - R_i\alpha_T\frac{\Sigma A_i\,\Delta T_i}{\Sigma A_i} + \alpha_T\,a\,\Delta T_s \qquad (56)$$

and, hence,

$$\sigma_\phi^{(R)} = \frac{E}{a-e+t}\,\bar{w}(x = L/2) \qquad (57)$$

$$\sigma_R^{(R)} = \frac{EA}{2(a-e+t)^2\cdot t_R}\,\bar{w}(x = L/2) \qquad (58)$$

IV. Numerical Results

Numerical results are obtained for geometric properties which are closely related to a preliminary Phase B tank design for a MDC Space Shuttle Orbiter.

The design values at a representative station are:

$h = 0.6$ in.	$L = 20$ in.
$b = 0.04$ in.	$R = 83$ in.
$t = 0.055$ in.	$E = 1.07 \cdot 10^7$ lb/in.^{2}
$s = 3.3$ in.	$\nu = 0.3$
$A = \Sigma A_i = 0.26$ in.^{2}	

For the compression side of the tank (due to overall vehicle loads) the axial line load was approximately $\bar{N}_x = -1000$ lb/in and the internal pressure was 30 lb/in^2. The temperature difference across the ring stiffener at $x = \pm L/2$ was assumed to be $T = 10^\circ$F.

Figure 5 shows the obtained variation of axial and hoop stresses between two ring stiffeners. It can be seen that bending of the axial stiffener due to the existence of the ring stiffener at $x = \pm L/2$ causes high compression stresses in the outer fiber of the axial stiffener. This could result in local crippling of the stiffener.

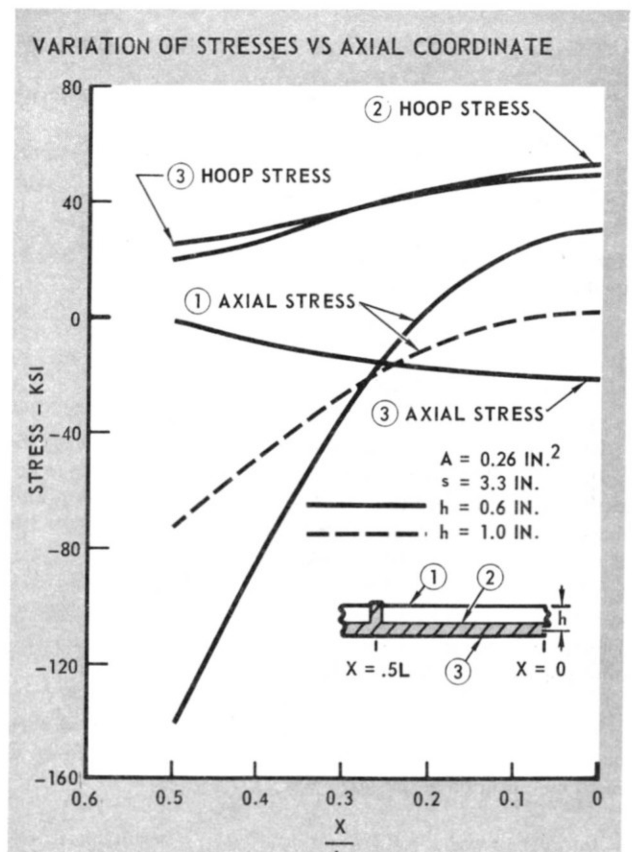

Figure 5

In addition to the results for h = 0.6 in. the case of a higher axial stiffener, h = 1.0 in., has been investigated. This modification results in a considerable reduction of the maximum stress level in the stiffener.

In figure 6 the effect of a reduction of the spacing of the axial stiffener is shown. The stress reduction is much less pronounced compared with the effect of increased stiffener height (figure 5), if equal amount of additional structural weight is considered.

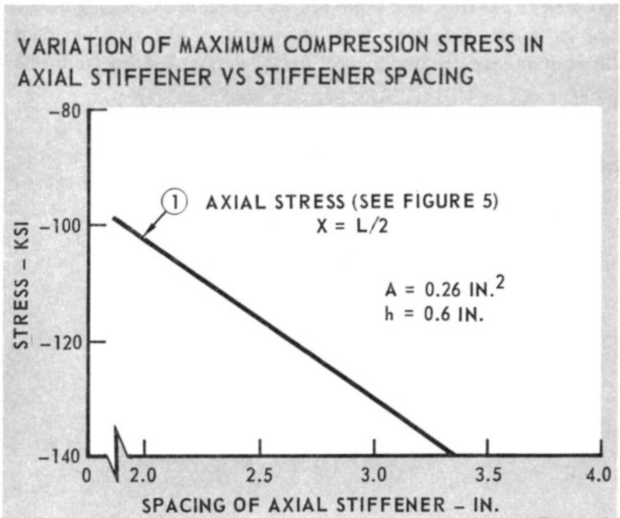

Figure 6

In figure 7 the influence of a reduction of the cross section area of the ring stiffener at $x = \pm L/2$ is demonstrated. Less circumferential stiffening yields considerably reduced bending stresses in the axial stiffeners.

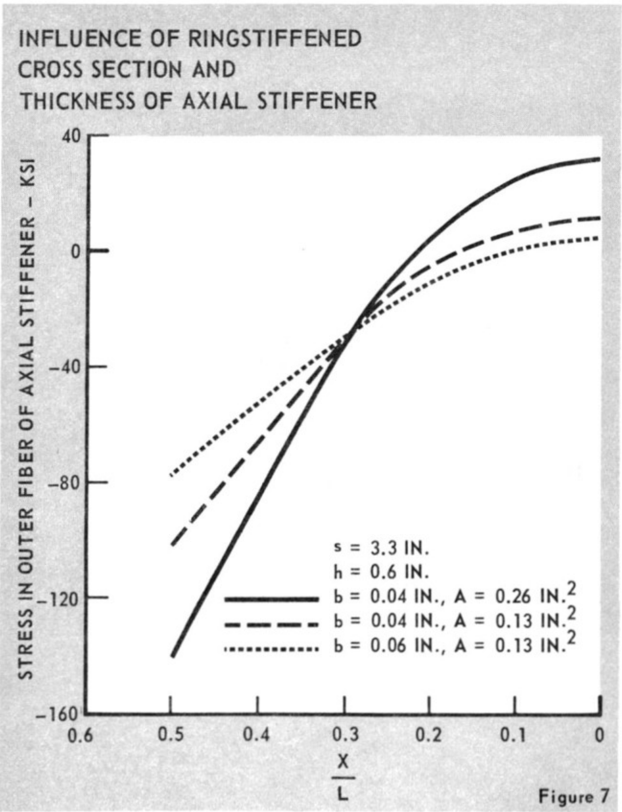

Figure 7

The effect of increased thickness of the axial stiffener is also shown in figure 7. Fifty percent increase of the thickness reduces the maximum stress from -103.19 ksi to 78.38 ksi. The first reduction of the maximum stress is accompanied by a weight saving; additional reduction requires a considerable amount of additional material.

In figure 8, the effect of an additional ring stiffener at station x = 0 has been investigated. This stiffener has a cross section area of A_s and no temperature variation throughout its cross section, since the radial extension of the stiffener is assumed to be small. It can be seen that the additional ring stiffener reduces the maximum stress in the axial stiffener.

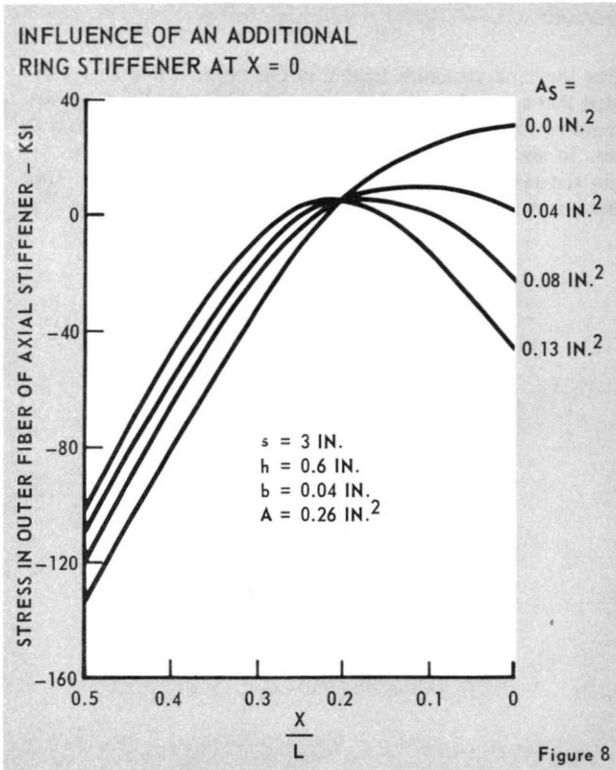

Figure 8

Finally, the distribution of the radial deflection is presented in figure 9. For these curves the stiffener spacing is 3.0 in. The smoothing effect of more rigid axial stiffeners is clearly revealed.

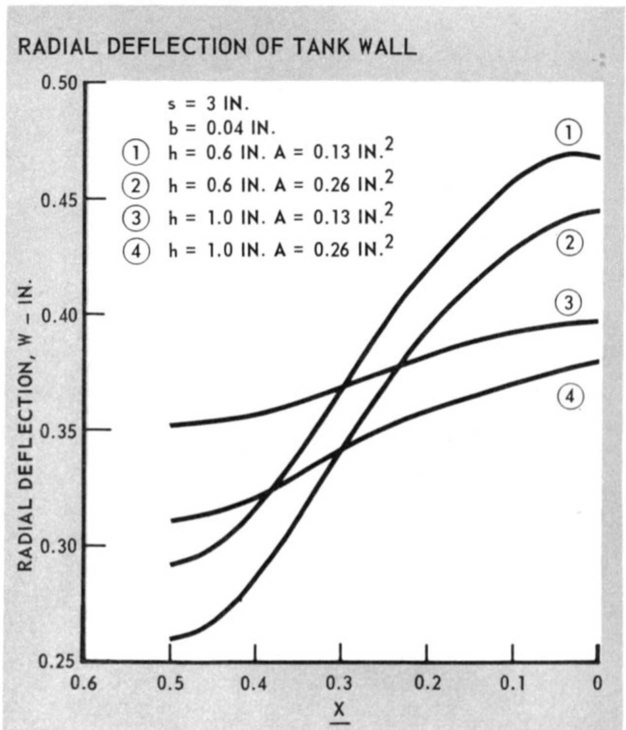

Figure 9

V. Conclusion

It has been demonstrated that heavily stiffened pressurized tanks require a detailed study of their discontinuity stresses. The "smearing-out" technique is not applicable for such structures and may lead to erroneous results. Accounting for axial load coupling ("beam column effect") was included and found to be important.

For the tank structure treated in this paper it had been concluded that a local increase in thickness (and eventually in height) is required for the axial stiffeners in the vicinity of the ring stiffener. In addition, the ring stiffener should be designed to restrain the tank from radial expansion as little as possible. This requirement creates no severe design problems, since the ring stiffeners are designed to introduce mainly shear loads into the tank structure.

An additional ring stiffener at $x = 0$ results in a comparatively high weight penalty. The same is true for reduced spacing of the axial stiffeners. Effect on total structural weight was less than 100 pounds, due to proper local design detail resulting from this study.

References

(1) W. Flügge, Stresses in Shells
Springer-Verlag, Berlin/
Heidelberg/New York, 1967